

Bis-(thiosemicarbazonato) Zn(II) complexes as building blocks for construction of supramolecular catalysts†

Vladica Bocokić,^a Martin Lutz,^b Anthony L. Spek^b and Joost N. H. Reek^{*a}

Received 3rd November 2011, Accepted 22nd December 2011

DOI: 10.1039/c2dt12096h

In this paper we report the application of bis-(thiosemicarbazonato) Zn(II) complexes as building blocks in the construction of supramolecular transition metal assemblies. We investigated their coordination behaviour towards pyridylphosphine molecules and found these systems comparable to those based on Zn (porphyrin) and Zn(salphen) complexes. Additionally, catalytic experiments and an *in situ* high-pressure FTIR study of the supramolecular rhodium hydroformylation catalysts, assembled using the bis-(thiosemicarbazonato) Zn(II) complexes, demonstrate their applicability in supramolecular catalysis and their potential for application in other areas of supramolecular chemistry.

1 Introduction

Supramolecular chemistry has evolved into a mature field of science and a plethora of fascinating nano-sized structures have been prepared by self-assembly. Whereas the initial focus was on the generation of complex nano-sized structures and understanding the principles involved in their formation, current research is more often associated with the introduction of information (function) into these supramolecules.^{1,2} There is increasing interest in the use of metal–ligand interactions as this strategy provides new opportunities for the introduction of function. In addition, metal–ligand interactions are ideal for the construction of supramolecular assemblies, since they are generally directional and tunable in strength therefore facilitating the design of structures with controlled geometries and dynamics. The supramolecular structures constructed utilising these interactions include metal-lodendrimers,³ molecular cages,^{4,5} catenanes and rotaxanes.⁶ The latter compounds were shown to be suited to the construction of molecular machines⁷ and such supramolecular structures can also be of value in the area of light harvesting devices.⁸

An important research field that has attracted enormous interest in recent years is that of controlled porous materials and metal–organic frameworks (MOFs). The interest in these materials is fuelled by (potential) application in separation techniques, gas (hydrogen) storage, recognition, sensing, and catalysis.^{9–23} Metalloporphyrins²⁴ provide versatile building

blocks for the construction of all types of supramolecular assemblies and they are also frequently used for the construction of porous solid materials.

In our group metalloporphyrins have been used as building blocks to encapsulate transition metal catalysts.^{25–27} Recently we also took advantage of the chromophoric character of porphyrins: the assembly of Zn(II)porphyrins onto a functionalised bis (thiolate)-bridged ([2Fe2S]) diiron-based hydrogenase catalyst led to a supramolecular complex that displayed photo-activity forming molecular hydrogen upon exposure to light in the presence of a proton source.²⁸

Since the supramolecular approach to catalyst exploration is very versatile we aimed at extending the concept to other building blocks. We demonstrated that the pyridyl analogues of classical BIAN-ligands could be used as the template ligand,²⁹ and we also showed that Zn(II)salphen building blocks can be used analogously to Zn(II)porphyrins.³⁰ These salphen building blocks were much easier to prepare and were more structurally varied than porphyrins, however, they were shown to be subject to *trans*- and demetallation.^{31,32}

We therefore continued our search for new building blocks and looked into the chemistry of dithiocarbazonates (Fig. 1) and complexes thereof.^{33,34} Much to our surprise these building blocks have not yet been studied as molecular building blocks in supramolecular chemistry.

In this paper we report the application of the bis-(thiosemicarbazonato) Zn(II) (Zn(btsc)) complexes as building blocks in supramolecular chemistry, *i.e.* their coordination chemistry with respect to pyridine and pyridylphosphines, as compared, to the Zn(II) building blocks we used previously. We show that bis-(thiosemicarbazonato) Zn(II) complexes are stable building blocks with coordination properties similar to Zn(II)porphyrins and Zn(II)salphens. To demonstrate their applicability in the construction of supramolecular transition metal catalysts, we applied these complexes as building units of supramolecular rhodium hydroformylation catalysts. With many heteroatoms in the

^aUniversity of Amsterdam, van't Hoff Institute for Molecular Sciences, Science Park 904, 1098 XH Amsterdam, The Netherlands. E-mail: J.N.H.Reek@uva.nl; Fax: (+31) (0)20 5255604; Tel: (+31) (0)20 5256437

^bUtrecht University, Faculty of Science, Bijvoet Center for Biomolecular Research, Crystal and Structural Chemistry, Padualaan 8, 3584 CH Utrecht, The Netherlands

† Electronic supplementary information (ESI) available. CCDC reference numbers 799011–799012. For ESI and crystallographic data in CIF or other electronic format see DOI: 10.1039/c2dt12096h

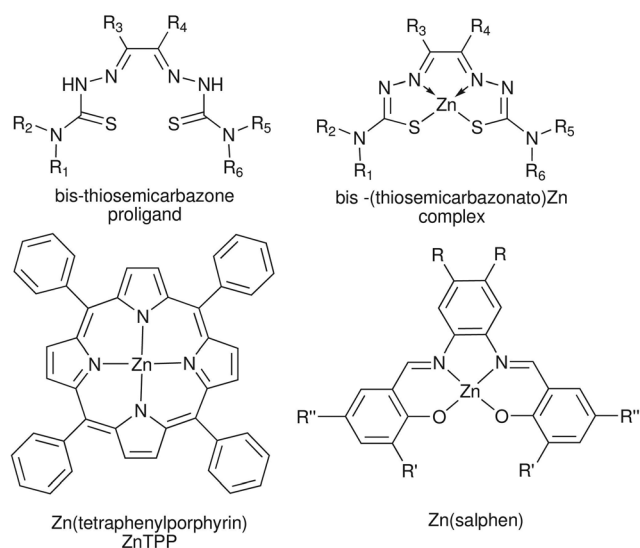


Fig. 1 Structure of bis-thiosemicarbazone proligand (top left) and its metal complex (top right). ZnTPP (bottom left) and Zn(salphen) (bottom right) are commonly used building blocks in supramolecular chemistry.

molecule, most notably sulfur, which may act as a catalyst poison, it is important to demonstrate the compatibility of the Zn (btsc) complexes with the transition metal atom. Formation of the catalyst and confirmation of its activity in hydroformylations are therefore important goals of this paper. By using *in situ* high-pressure infrared spectroscopy we show the formation of the bis-phosphine ligated rhodiumhydrido species, commonly formed under hydroformylation conditions. The catalytic activity of this species, was evaluated using a showcase set of linear terminal and internal alkenes as substrates in catalysis. The results of our investigations suggest a great potential for application of these Zn(II)btsc complexes in the area of supramolecular chemistry, which herein is demonstrated with examples in the area of supramolecular catalysis.

2 Results and discussion

Tetradentate bis-thiosemicarbazone (btsc) (pro)ligands and their transition metal complexes have been known for over 50 years.³⁴ The exceptional stability of these complexes, manifested in reversible protonation of the amido side arms but not demetallation upon treatment with concentrated sulfuric (phosphoric and perchloric as well) acid, was exploited by using these protonated metal complexes as cations in synthesis of complex salts.³⁵ In our stability experiment, we exposed it to conditions under which demetallation of the Zn(II)salphen, occurred easily.³² Contrary to Zn(II)salphen,† no demetallation was observed when 3 equivalents of benzimidazole and a Zn(btsc) complex were mixed, neither upon mixing, nor after 18 h of heating at 75 °C (see Experimental section). Besides being highly stable, their (transition) metal complexes are biologically active and many studies have shown that they display antitumor, antibacterial and antiviral properties.^{36–38} Potential medical application could be found in the affinity of Cu(II)(btsc) complexes towards oxygen-poor (cancer) tissue, and applications of M(II)(btsc) complexes (M = Zn, Cu) as tumour marker agents have already been demonstrated.^{39–42}

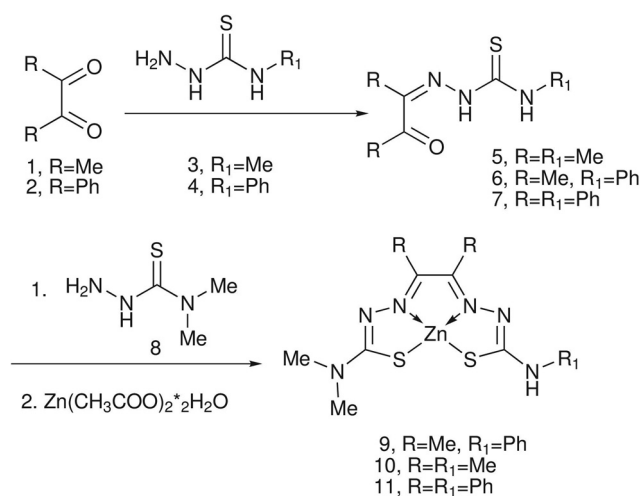


Fig. 2 One-pot two-step protocol for the synthesis of dissymmetric Zn (btsc) complexes.

2.1 Synthesis

The preparation of M(II)(btsc) complexes is rapid and facile. A typical synthesis protocol consists of two steps: preparation of the (pro)ligand by condensation of a dicarbonyl compound with two thiosemicarbazide molecules, followed by metallation with an appropriate metal salt.^{43,44} Condensation of two different thiosemicarbazides to a dicarbonyl (leading eventually, to dissymmetric M(btsc) complexes), can also be performed, but a good control of reaction conditions during synthesis, is required to avoid formation of unwanted side products.⁴⁵

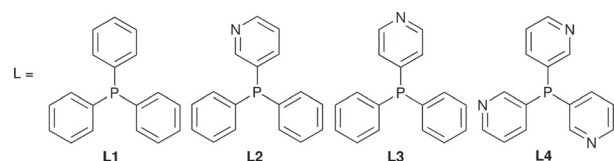
For our syntheses we used a slightly modified synthetic procedure as we did not isolate any of the intermediates. The condensation and metallation were performed in a one-pot two step protocol under very mild conditions, as shown in Fig. 2. For this initial study three exemplary dissymmetric Zn(btsc) complexes **9–11** with different peripheral substituent sizes were prepared in good to high yields (70–80%) and purity, (≥95% by NMR).

2.2 Coordination studies

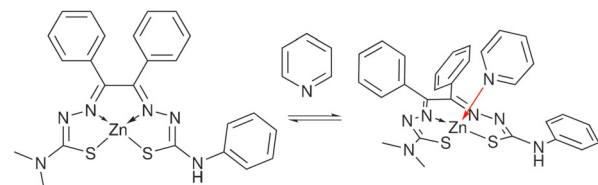
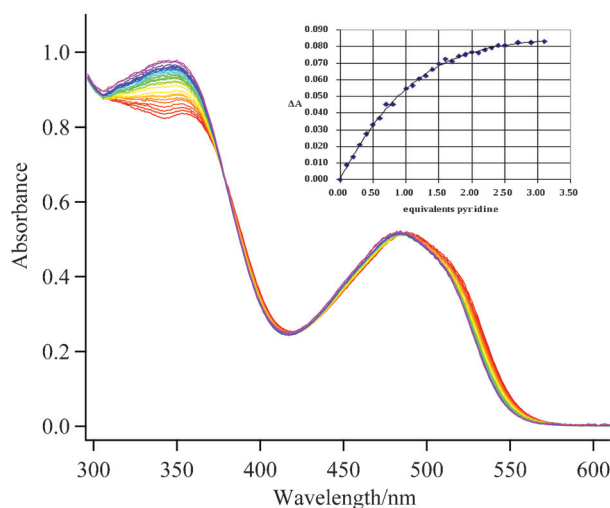
2.2.1 Assembly in solution. The essential element of the ligand–template approach for encapsulation of transition metal catalysts is the coordination of a pyridyl moiety to the Zn(II) centre.⁴⁶ The strength of this association is therefore crucial for successful assembly formation, and for low (catalytic) concentrations the association constant should be high.

The association constant of pyridine to a Zn(II) building block is often used as a guideline value for the family of similar systems. By performing a UV-Vis titration of the complex **11** with pyridine (see Fig. 3) we found that their association constant falls roughly in the order of magnitude of the Zn(II) salphen–pyridine interaction, with $K = 1.6 \times 10^5 \text{ l mol}^{-1}$.^{26,47–49} This high K value makes the Zn(btsc) complexes interesting for the application as supramolecular building units.^{50,51}

2.2.2 Assemblies in the solid state. To further confirm the coordination of the phosphine–pyridyl ligands§ to these Zn(II) building blocks, the coordination complexes were crystallized



(a) Phosphorus ligands used in this study.

(b) Coordination equilibrium. $K = 1.6 \cdot 10^5 \text{ M}^{-1}$.

(c) UV-Vis Spectra and the titration curve.

Fig. 3 UV-Vis changes during titration are small, but sufficient to produce a well-behaved titration curve (insert), which was used to calculate the association constant.

from toluene solution by hexane diffusion *via* the gas-phase. The crystal structures of assemblies of complex **9** with 3- and 4-(diphenylphosphino)-pyridine (**L2** and **L3** Fig. 3a) show axial coordination of the pyridyl moiety to the Zn(II) centre, which adopts a square-pyramidal geometry bending slightly out of the SNNS-plane (see Fig. 4). Importantly, the lone pair of either phosphorus atom is not involved in coordination, and therefore could be used for coordination to (soft) transition metals in the construction of supramolecular catalysts. An interesting feature of both assemblies is formation of dimeric structures *via* two N–H...S bonds per dimeric unit, similar to Zn(btsc) dimers Alsop *et al.* reported (Fig. 4).⁵² The N...S distances of atoms involved in hydrogen bonding are typical for such structures (3.702(11) Å in **9·L2** and 3.463(4) Å in **9·L3**).⁵² Small inserts in Fig. 4 display stacking of the Zn(btsc) complexes with distance between the Zn–N–CC–N planes of the two stacking units around 3.5 Å (3.560(4) Å in **9·L2** and 3.5295(18) Å in **9·L3**), suggesting existence of “ π – π ” interactions, not unusual between layers of flat aromatic molecules.^{53,54} In these dimers the Zn(btsc) complexes are almost perfectly coplanar while the pyridylphosphine moieties coordinate to Zn centres on opposite sides

of, the plane defined by the two complexes. This 2 : 2 assembly, is strikingly similar to a 1 : 2 assembly Kuil *et al.* reported, where two **L2** molecules coordinate to Zn centres on opposite sides of a bis-Zn(II)–salphen complex.⁴⁹ The Zn...Zn distances in the current structures are 8.7803(8) Å (**9·L3**) and 9.185(2) Å (**9·L2**) which is similar to the Zn...Zn distance in the 1 : 2 assembly. It would be interesting to use these self-assembled dimers as template to bring two pyridylphosphines together. However there is no evidence yet that such structures form N–H...S bonds in solution, as we did not observe any effect typical for formation of a supramolecular bidentate ligand on a bis-Zn platform in asymmetric hydroformylation of styrene, as was described previously.⁴⁹

2.3 *In situ* high-pressure infrared spectroscopy and catalysis

The assemblies of Zn(btsc) complexes with **L2–L4** are essentially monodentate ligands, with unconventional steric bulk remote from the phosphorus atom and the transition metal. They are also electronically different from a typical monodentate ligand PPh_3 (**L1**) and it was anticipated that the combination of the unusual steric and electronic properties of these ligands would have an impact on catalysis.

In a typical hydroformylation experiment $\text{Rh}(\text{acac})(\text{CO})_2$ and the ligands are mixed *in situ* to form the active species.[¶] We monitored the formation of rhodium supramolecular catalyst *in situ* from $\text{Rh}(\text{acac})(\text{CO})_2$, tris-(*m*-pyridyl)phosphine **L4**, and the Zn(btsc) complex **9**,^{||} using infrared spectroscopy.^{57,58} The IR spectrum we obtained is similar to that of the triphenylphosphine analogue. Four bands of similar intensities at 2071, 2056, 2005 and 1970 cm^{-1} were observed, indicating formation of the *ee* and *ea* isomers (Fig. 6) in approximately equimolar amounts.⁵⁹

The shoulder at about 1920 cm^{-1} might be the rhodium-hydride (Rh–H) stretch, which is very rarely observed due to its weak intensity.⁶⁰

For comparison, application of ZnTPP instead of Zn(btsc) leads exclusively to the formation of the mono-ligated rhodium complex, since the assembly **L4·(ZnTPP)**₃ is so large that only one phosphorus can coordinate to rhodium.²⁵

This indicates that the significant difference in size between the Zn(btsc) and ZnTPP is reflected in the phosphine coordination mode allowing formation of the bis-phosphine rhodium species with Zn(btsc) as building block.

The molecular modelling figure of the *ea* and the *ee* isomers, Fig. 7, shows that there is no significant steric hindrances between the various building blocks in the bisphosphine rhodium species. Numerous phosphine conformations and large rotational freedom around the N–Zn coordinative bond convey rather considerable flexibility to the assembly allowing facile avoidance of steric crowding.

That these rhodium species were also active catalysts for hydroformylation was confirmed by addition of substrate to the IR autoclave. Injection of 1-octene into the autoclave triggered the immediate start of catalysis, with an initial turnover frequency (TOF) of about 60 h^{-1} , which is significantly faster than observed with triphenylphosphine under similar conditions (4–15 h^{-1}).^{26,30,61} The four carbonyl bands of the rhodium

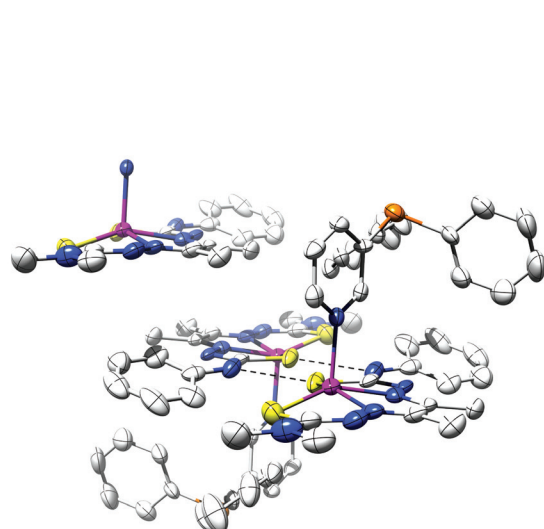
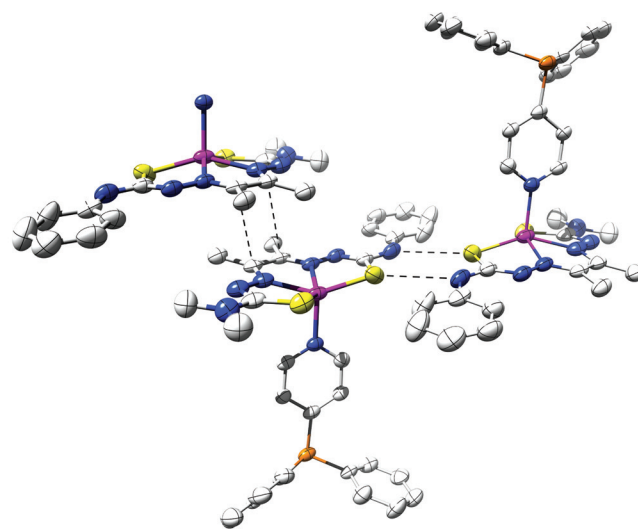
(a) [9-L2]₂ dimer and $\pi - \pi$ stacking(b) [9-L3]₂ dimer and $\pi - \pi$ stacking

Fig. 4 Solid state structures of the extended assemblies. Thermal motion ellipsoids drawn at 50% probability. H atoms and co-crystallised solvent molecule (toluene in **9-L3**) have been removed for clarity. Colour legend: C = white, N = blue, S = yellow, P = orange and Zn = magenta. Dimeric super-structures are formed *via* a pair of N–H–S hydrogen bonds. Pyridylphosphines coordinate on opposite sides of the [Zn(btsc)]₂-plane. $\pi - \pi$ stacking shown in small inserts.

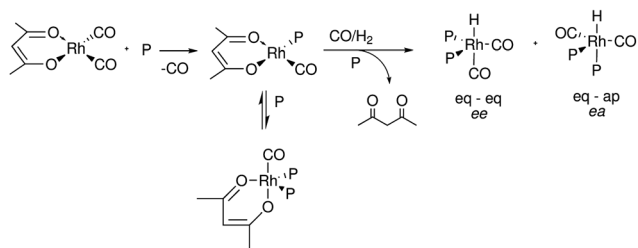


Fig. 5 Generally accepted rhodium hydroformylation catalyst activation under syngas atmosphere.⁵⁵

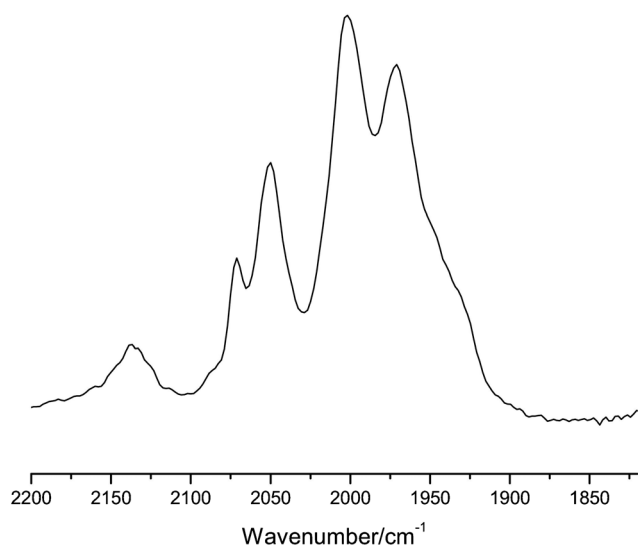


Fig. 6 Carbonyl region of the *in situ* IR spectrum showing the four bands of the *ee* and *ea* rhodium isomer mixture. The weak band at 2135 cm⁻¹ is the free CO, and the shoulder at around 1920 cm⁻¹ might be the Rh–H stretch, *p* = 20 bar, CO/H₂ = 1 : 1, *T* = 40 °C.

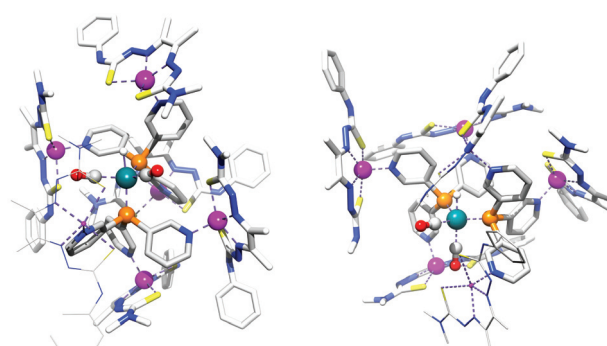
(a) *ea* isomer(b) *ee* isomer

Fig. 7 Molecular models (PM3, Spartan) of the *ea* and the *ee* rhodium-hydrido complexes. Although bulky, the supramolecular ligand allows formation of bis-ligated rhodium species. Colour legend: C = white (in **9**) or grey, H = white ball, O = red, N = blue, P = orange, Zn = magenta and Rh = turquoise; for clarity, Zn(btsc) molecules were rendered partly as wire.

species did not change during catalysis, showing that the rhodium hydride complexes were the resting state of the catalyst. This, together with the rate order in respect to the substrate being 1 (see insert in Fig. 8), indicated that the hydroformylation follows type I kinetics.**

A more extensive set of catalytic experiments was performed using Zn(btsc) complexes **9–11**, ligands **L1–L4**, and substrates shown in Fig. 9. As expected, the conversions of internal alkenes were lower than those of terminal alkenes for all catalytic systems. Additionally, the PPh₃-based rhodium catalysts displayed lower conversions than those with pyridyl–Zn(btsc) moieties. The conversion was higher because the phenyl groups on P were replaced by pyridyl–Zn(btsc) motifs see Fig. 10, reflecting the increasing withdrawal of the electronic density from

rhodium. Unexpectedly, the presence of three equivalents of Zn(btsc) **9** in hydroformylation experiment using **L1**, (entries 2, 12, and 24 in Table 1), which has no positions for Zn(btsc) coordination, has also led to conversion higher than achieved only with **L1**. Importantly, these experiments ultimately show that not only the Zn(btsc) complexes do not poison the catalyst, but that their presence is actually beneficial for catalysis, even if there is no ligand-provided coordination site as in **L2–L4**. The origin of this effect is not clear yet, however, it is possible that the Zn(btsc) complexes contribute to electron-depletion of the rhodium centre. The Zn(II) centre may coordinate to the O of a Rh-associated carbonyl functionality,^{††} withdrawing electron density *via* the σ bonds. In experiments with Zn(btsc)·**L2–L4**, the pyridyl-phosphine itself is electron-poorer than PPh₃ due to the electronegative nitrogen atom in the ligand; additionally, coordination of Zn(btsc) complexes to N leads to further electron-depletion of the ligand and rhodium centre. In consequence, conversion numbers in experiments with the supramolecular ligands are higher than those achieved using PPh₃ or PPh₃/Zn(btsc) system.

Generally accepted⁶² effects of reduced back-donation from Rh to the coordinated CO or alkene are:

- facilitated CO dissociation from the rhodiumhydrido resting state and entry of the catalyst into the catalytic cycle

- weaker back-donation from Rh to the coordinated alkene, facilitating rotation around Rh–alkene σ -bond and lowering the hydride migration barrier.

Such effects directly cause higher catalytic activity, but also higher alkene isomerisation rate. This is well documented in the case of phosphites, which display both effects (increase of isomerisation and hydroformylation rate).^{63–68} In our case, the electronic effects are much smaller than with the phosphites, and we only see a slight increase in conversion. Decreased back-donation to the antibonding CO-orbitals leads to stronger CO bonds of the coordinated CO molecules and as a consequence to higher frequencies of the CO vibrations in the IR spectrum.⁶⁹ Indeed we find this experimentally: the HP-IR spectrum of the PPh₃-based rhodium catalyst displays bands 15–30 cm^{−1} lower than the supramolecular catalyst (PPh₃: 2055, 2030, 1989 and 1941 cm^{−1}; **L4·9**₃: 2071, 2056, 2005 and 1970 cm^{−1}, see comparison of spectra in Fig. 12, Experimental section).

Similar wavenumber differences were previously reported with systems using xantphos ligands bearing substituents with various electron-withdrawing properties.⁵⁶

The selectivity of the current encapsulated catalyst is virtually identical to PPh₃-based rhodium catalysts. Thus, the application of Zn(btsc) building blocks for supramolecular rhodium catalysts

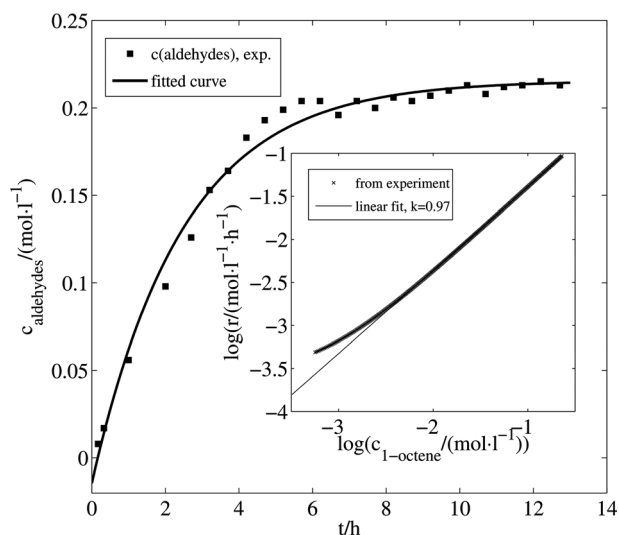


Fig. 8 Hydroformylation of 1-octene is typical for type I kinetics, with the rate order in respect to the substrate being 1 (here 0.97, see insert).

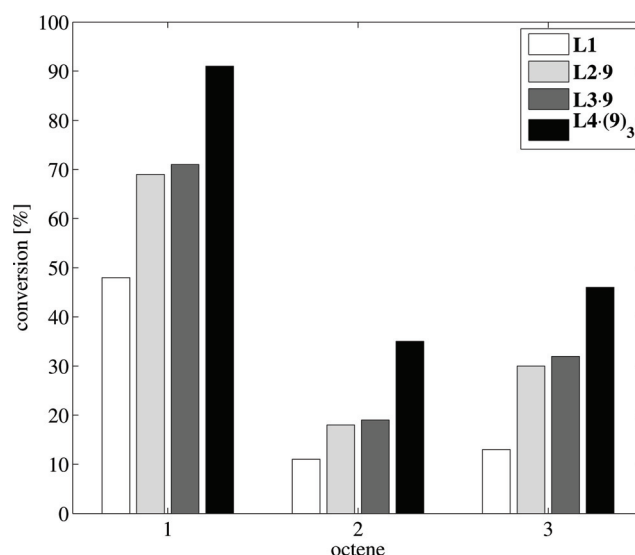


Fig. 10 Comparison of octene hydroformylation with various ligands. Conversions are higher in systems containing more [Zn(btsc)–pyridyl] moieties.

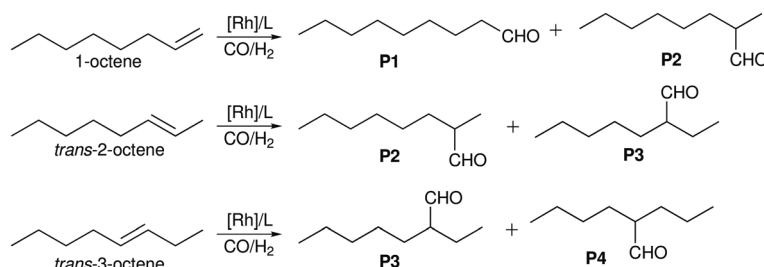


Fig. 9 Hydroformylation of 1-, *trans*-2- and *trans*-3-octene.

Table 1 Hydroformylation of terminal and internal octenes

Entry	Alkene	Ligand	Zn(btsc)	[Zn]/[L]	Conv. (%)	Iso. (%)	P1	P2	P3	P4	Pn/P(n+1)
1	1-octene	L1	—	—	48	1.1	74	25	—	—	3.0
2	1-octene	L1	9	3	60	1	75	24	—	—	3.1
3	1-octene	L2	9	1	69	≤0.1	69	31	—	—	2.2
4	1-octene	L2	—	—	55	1	73	26	—	—	2.8
5	1-octene	L3	9	1	71	≤0.1	70	30	—	—	2.3
6	1-octene	L3	—	—	57	1	74	25	—	—	2.9
7	1-octene	L4	—	—	63	1.2	75	24	—	—	3.1
8	1-octene	L4	9	3	91	0.4	69	30	—	—	2.3
9	1-octene	L4	10	3	84	0.4	73	27	—	—	2.7
10	1-octene	L4	11	3	89	0.5	70	29	—	—	2.4
11	2-octene	L1	—	—	11	≤0.1	—	56	44	—	1.27
12	2-octene	L1	9	3	17	≤0.1	—	55	45	—	1.27
13	2-octene	L2	9	1	18	≤0.1	—	56	44	—	1.27
14	2-octene	L2	—	—	13	≤0.1	—	56	44	—	1.27
15	2-octene	L3	9	1	19	≤0.1	—	57	43	—	1.32
16	2-octene	L3	—	—	12	≤0.1	—	56	44	—	1.27
17	2-octene	L4	—	—	21	≤0.1	—	56	44	—	1.27
18	2-octene	L4	9	3	35	≤0.1	—	59	41	—	1.44
19	2-octene	L4	10	3	27	≤0.1	—	56	44	—	1.27
20	2-octene	L2	11	1	23	≤0.1	—	56	44	—	1.27
21	2-octene	L3	11	1	22	≤0.1	—	56	44	—	1.27
22	2-octene	L4	11	3	34	0.2	—	56	44	—	1.27
23	3-octene	L1	—	—	13	≤0.1	—	—	50	50	1.00
24	3-octene	L1	9	3	19	≤0.1	—	—	50	50	1.00
25	3-octene	L2	9	1	30	≤0.1	—	—	50	50	1.00
26	3-octene	L3	9	1	32	≤0.1	—	—	50	50	1.00
27	3-octene	L4	—	—	24	≤0.1	—	—	50	50	1.00
28	3-octene	L4	9	3	46	≤0.1	—	—	50	50	1.00
29	3-octene	L4	10	3	38	≤0.1	—	—	50	50	1.00
30	3-octene	L4	11	3	39	≤0.1	—	—	50	50	1.00

Conditions: [Rh] = 0.70 mmol l⁻¹, [P]/[Rh] = 5.0, [Zn]/[equiv. pyridyl group] = 1.0, [1-octene]/[Rh] = 1000, 16 h; [*trans*-2-octene]/[Rh] = [*trans*-3-octene]/[Rh] = 500, 24 h; *T* = 40 °C, *p* = 20 bar, CO/H₂ = 1 : 1. No base added.

leads to increased conversions in hydroformylation of terminal and internal octenes, while preserving the selectivity typical for PPh₃-based catalysts.

3 Summary and conclusion

We have studied the application of a small set of bis-(thiosemicarbazonato) Zn(II) complexes as building blocks for construction of supramolecular complexes; in particular as building blocks that associate to ligand-templates to encapsulate transition metal complexes for catalysis. The coordination behaviour of these complexes is similar to that of Zn(II)-salphens, with the pyridine-Zn(btsc) association constant of $K = 1.6 \times 10^5$ l mol⁻¹, two orders of magnitude higher than those displayed by related Zn(II)porphyrin-pyridine systems. In addition, the current complexes are significantly more stable than the Zn(II)-salphen complexes, especially concerning demetallation under acidic conditions.

Under syngas atmosphere, the supramolecular ligands formed by these bis-(thiosemicarbazonato) Zn(II) complexes and trispyridyl-phosphine ligand building blocks react with a rhodium precursor giving active hydroformylation catalysts that display type I kinetics. According to HP-IR the encapsulation does not lead to phosphine dissociation as bisphosphine complexes are formed. The selectivity obtained in the hydroformylation of linear alkenes is typical for the PPh₃-based rhodium catalysts, however, the activity is about four times higher than that

observed with PPh₃. The differences in reactivity are likely due to electronic properties, as the supramolecular ligands are more electron-deficient than PPh₃.

We have thus successfully demonstrated the applicability of Zn(btsc) complexes as building blocks for the construction of supramolecular ligand assemblies and rhodium hydroformylation catalysts thereof. A particularly interesting aspect, and a great potential of these complexes, is their structural variability and possibility for post-synthetic modifications. The opportunity to access a stable building block that is easy to modify makes these compounds very attractive for further exploration in supramolecular chemistry, also including applications other than catalysis.

4 Experimental

Solvents used for the syntheses of Zn(btsc) complexes were used as obtained from supplier. Solvents used in catalytic, spectroscopic (HP-FTIR, UV-Vis) and crystallisation experiments were dried and freshly distilled prior to use: toluene and hexane were distilled over Na, CH₂Cl₂ over CaH₂. All deuterated solvents except DMSO were prepared by freeze-pump-thaw technique and kept under 3–4 Å molecular sieves. Reagents **1–3**, **7**, **8**, **L1** and Zn(CH₃COO)₂·2H₂O were purchased from Aldrich and used without further purification. Substrates for catalysis and high-pressure IR were degassed by dinitrogen bubbling and filtered over a short plug of alumina prior to use. Phosphine ligands were prepared according to the previously published

procedures.⁷⁰ NMR spectra were acquired on the Varian Mercury-VX 300, Bruker DRX300 (¹H at 300 MHz, ³¹P at 100 MHz, and ¹³C at 75 MHz), and Bruker ARX400 (¹H at 400 MHz, ³¹P at 125 MHz, and ¹³C at 100 MHz). The resonances are referenced to solvent itself as an internal standard and are reported in parts per million (ppm). Mass spectrometry (MS) measurements were performed using a fast atom bombardment (FAB) ionisation mode. IR spectra were recorded on the Nicolet Nexus 670 FT-IR spectrometer operated by Omnic 6.2 Software; UV-Vis, measurements were performed on the Hewlett–Packard 8453 spectrometer; gas chromatography (GC) analysis were done on the Shimadzu GC-17A chromatograph equipped with an FID detector using a 30 mm long column with 0.32 mm diameter and dimethylsiloxane cross-linked phase of 3 µm thickness. Catalytic experiments were performed in mini-4-autoclaves connected to the same high-pressure line, allowing all four reactions to be ran under the same pressure. Before each run the autoclaves were evacuated, flushed with nitrogen, and tested for leaks at *ca.* 35 bar syngas. Molecular graphics images were produced using the UCSF Chimera package from the Resource for Biocomputing, Visualization, and Informatics at the University of California, San Francisco.⁷¹

4.1 Syntheses

4.1.1 Compound 5. It was prepared as described by Cowley *et al.*⁴³ Thiosemicarbazide **3** (1.00 g, 9.51 mmol) was dissolved in water (17 ml) and treated with 5.5 ml conc. HCl at 10 °C in a 100 ml round-bottom flask. A cooled solution of diketone **1** (1.0 ml, 11.85 mmol) in water (20 ml) was added dropwise under vigorous stirring, with white bulky precipitate forming immediately. After 2 h of stirring under ice cooling, the product was collected by filtration, washed twice with 20 ml cold water, once with 15 ml of cold diethyl ether and dried in air. Yield: 1.33 g (81%) of white powder. NMR analysis of the product showed ≥95% purity and it was used further without additional purification. ¹H NMR (300 MHz, DMSO-*d*₆, 25 °C): δ 10.63 (s, 1H, NH), 8.61 (s, br, 1H, CH₃NH), 3.04 (s, br, 3H, CH₃NH), 2.40 (s, 3H, CH₃CO), 1.94 (s, 3H, CH₃CN). ¹³C{¹H} NMR (75 MHz, DMSO-*d*₆, 25 °C): δ 197.2 (C=O), 178.6 (C), 145.2 (C), 31.1 (CH₃), 24.5 (CH₃), 9.7 (CH₃). MS (FAB+): *m/z* = 173.0491 found, calculated: 173.0600.

4.1.2 Compound 6. Prepared analogously to compound **5**. Thiosemicarbazide **4** (2.51 g, 15.00 mmol) was partially dissolved in water (60 ml) and treated with 0.5 ml 6 M HCl at 10 °C in a 200 ml round-bottom flask. A cooled solution of **1** (1.65 ml, 18.75 mmol) in water (30 ml) was added dropwise to the solution of **4** under vigorous stirring. White bulky precipitate formed immediately. More water (50 ml) was added to facilitate stirring. After 1.5 h of stirring under ice cooling, the product was collected by filtration, washed twice with 30 ml cold water, once with 25 ml of cold diethyl ether and dried in air. Yield: 3.23 g (91%) of white powder. NMR analysis showed the product purity ≥95%. It was used further without additional purification. ¹H NMR (300 MHz, DMSO-*d*₆, 25 °C): δ 10.34 (s, 1H, NH), 9.82 (s, 1H, NH), 7.59 (d, ³*J* = 7.6 Hz, 2H, H_{Ar}), 7.36 (t, ³*J* = 7.4 Hz, 2H, H_{Ar}), 7.15 (t, ³*J* = 7.4 Hz, 1H, H_{Ar}), 1.99 (s, 3H, CH₃), 1.07 (s, 3H, CH₃). ¹³C{¹H} NMR (75 MHz, DMSO-*d*₆,

25 °C): δ 175.7 (C=O), 152.1 (C), 138.4 (C), 127.5 (2C), 127.4, 124.3 (3C), 24.5 (CH₃), 17.4 (CH₃). MS (FAB+): *m/z* = 235.0663 found, calculated: 235.080.

4.1.3 Compound 7. This compound was prepared as described by Bost and Smith.⁷² Benzil, **2**, (2.00 g, 9.51 mmol), and thiosemicarbazide **4** (1.60 g, 9.51 mmol) were treated with 1 ml of glacial acetic acid in ethanol under reflux for 2 h. A creamy precipitate formed upon cooling which was collected, by filtration, washed with ice-cold ethanol (3 × 10 ml) and dried *in vacuo*. Yield: 2.33 g (86%) of fine white powder. NMR analysis showed ≥95% purity. The product was used further without additional purification. ¹H NMR (300 MHz, DMSO-*d*₆, 25 °C): δ 12.23 (s, 1H, NH), 8.45 (s, 1H, NH), 7.62 (d, ³*J* = 7.4 Hz, 2H, H_{Ar}), 7.39–7.14 (m, 12H, H_{Ar}), 6.11 (d, ³*J* = 7.4 Hz, 1H, H_{Ar}). ¹³C{¹H} NMR (75 MHz, DMSO-*d*₆, 25 °C): δ 170.8 (C=O), 146.1, 140.9, 138.8, 134.3, 132.1, 131.5, 130.4, 129.6, 129.5, 128.7, 128.1, 127.8 (2C), 127.7 (4C), 127.6, 127.1, 126.5 (C). MS (FAB+): *m/z* = 359.1096 found, calculated: 359.1100.

4.1.4 Complex 9. This complex was prepared according to procedure described by Cowley *et al.*⁴³ Compound **8** (253 mg, 2.12 mmol) was dissolved in tetrahydrofuran (THF) and treated with glacial acetic acid (0.2 ml) for *ca.* 20 min. **6** (500 mg, 2.12 mmol) was added to the solution and the mixture was stirred at room temperature next 3 h. Zinc(II) acetate dihydrate (559 mg, 2.54 mmol) was dissolved in 15 ml methanol and then added to the reaction mixture, followed by triethylamine (0.74 ml, 5.30 mmol). After stirring overnight at room temperature the solvents were evaporated and the residue suspended in *ca.* 10 ml methanol. The yellow solid was filtered off, washed with methanol (3 × 5 ml) and dried *in vacuo*. Yield: 647 mg (76%) of yellow powder, whose purity was estimated ≥95% by NMR. ¹H NMR (300 MHz, DMSO-*d*₆, 25 °C): δ 9.35 (s, 1H, NH), 7.57 (dd, ³*J* = 8.2 Hz, ⁵*J* = 1.2 Hz, 2H_{Ar}), 7.31 (t, ³*J* = 8.0 Hz, 2H, 2H_{Ar}), 7.04 (dt, ³*J* = 7.6 Hz, ⁵*J* = 1.2 Hz, H_{Ar}), 3.23 (s, 6H, N(CH₃)₂), 2.31 (s, 6H, CH₃), 2.25 (s, 6H, CH₃). ¹³C{¹H} NMR (75 MHz, DMSO-*d*₆, 25 °C): δ 178.2, 172.4, 149.1, 144.0, 141.2, 128.3 (2C), 121.2, 119.7 (2C), 39.6 (2C), 14.7, 13.8. MS (FAB+): *m/z* = 399.0396 found, calculated: 399.0404.

4.1.5 Complex 10. This complex was prepared analogously to complex **9** from **8** (119 mg, 1.00 mmol), **5** (173 mg, 1.00 mmol), and Zn(II) acetate dihydrate (231 mg, 1.05 mmol); glacial acetic acid and triethylamine were added in corresponding amounts as described above. Yield: 260 mg (77%) of yellow powder, NMR purity ≥95%. ¹H NMR (300 MHz, DMSO-*d*₆, 25 °C): δ 7.20 (s br, 1H, NH), 3.17 (s, 6H, N(CH₃)₂), 2.81 (s, 3H, NHCH₃), 2.17 (s, 6H, 2 × CH₃). ¹³C{¹H} NMR (100 MHz, DMSO-*d*₆, 25 °C): δ 178.0 (2C), 145.0 (2C), 48.9, 29.6 (2C), 14.2, 14.1. MS (FAB+): *m/z* = 337.6256 found, calculated: 337.6300.

4.1.6 Complex 11. The reactants **8** (50 mg, 0.42 mmol) and **7** (151 mg, 0.42 mmol) were stirred in THF (*ca.* 7 ml) at 50 °C for 2 h. The reaction mixture was cooled to room temperature, then Zn(II) acetate dihydrate (92 mg, 0.46 mmol) dissolved in 5 ml methanol was added. After stirring over night at room temperature the solvents were evaporated, the red residue was suspended in *ca.* 5 ml cold methanol, filtered off, washed twice

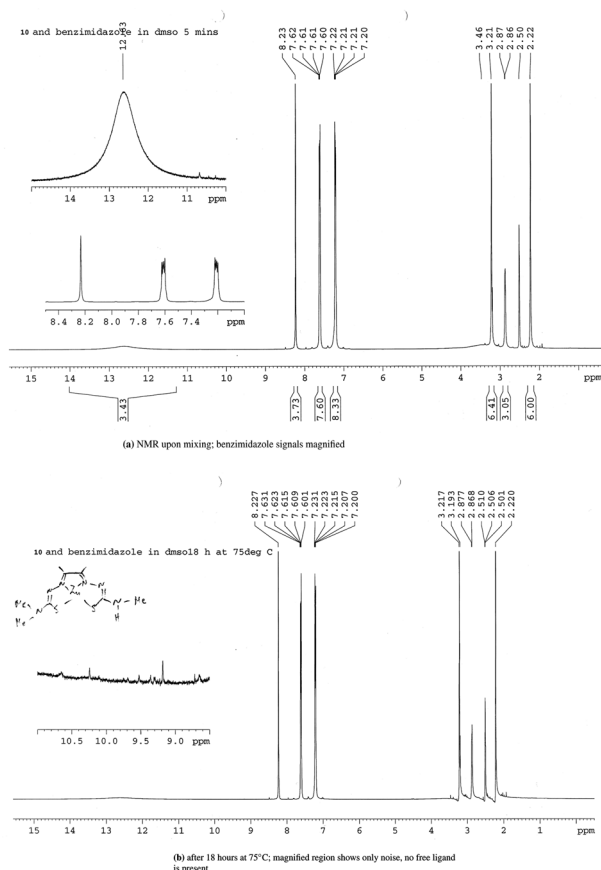


Fig. 11 NMR spectra showing that neither demetallation nor decomposition occur when benzimidazole is heated with the Zn(btsc) complex **10**.

with methanol and dried under vacuum. Yield: 150 mg (68%) of a bright red solid, NMR purity $\geq 95\%$. ^1H NMR (300 MHz, DMSO-*d*₆, 25 °C): δ 9.47 (s, 1H, NH), 7.60 (d, 3H, $J = 8.0$ Hz, 2H, H_{Ar}), 7.34–7.19 (m, 10H, H_{Ar}), 7.08 (t, $^3J = 7.8$ Hz, 2H, H_{Ar}), 6.83 (t, $^3J = 7.7$ Hz, 2H, H_{Ar}), 3.17 (s, 6H, N(CH₃)₂). ^{13}C { ^1H } NMR (75 MHz, DMSO-*d*₆, 25 °C, δ): 180.4, 173.7, 150.2, 143.8, 141.4 (2C), 134.8 (2C), 134.0 (2C), 130.8 (2C), 130.5 (2C), 129.1, 128.8 (2C), 128.0 (2C), 127.8, 122.2, 120.6, 39.6 (2C). MS (FAB⁺): $m/z = 522.0586$ found, calculated: 522.0600.

4.1.7 Stability test. The complex **10** (0.075 mmol, 25.3 mg) was mixed with benzimidazole (4 equiv. (35.44 mg) in DMSO-*d*₆, and 5 equiv. (44.30 mg) in acetonitrile-*d*₃). NMR spectra were recorded immediately at room temperature, and after 18 h at 75 °C.

No colour change, precipitation or appearance of the free ligand signals in NMR (Fig. 11) were observed in these experiments, indicating that no demetallation or other decomposition, reactions took place.

4.2 Crystallographic analysis

4.2.1 Crystallisation procedure. The procedure was the same for both assemblies. Equimolar amounts of Zn(btsc) **9** and ligand (**L2** or **L3**) were weighed in 5 ml Schlenk-tubes equipped

with stirring bars, and set under a dinitrogen atmosphere. To them *ca.* 3 ml toluene was added and the mixture was warmed to 50 °C under stirring. Additional toluene was added until everything was fully dissolved. The hot solution was quickly filtered through an HPLC filter into a Pasteur pipette (ca 1.2 ml), in a tall Schlenk-tube, all under dinitrogen. Hexane was added (*ca.* 15 ml) into the bottom of the Schlenk-tube (outside of the pipette), which was then tightly closed. It was kept at ambient temperature and protected from light. After two weeks first crystals appeared on inner wall of the pipette (the upper part), which grew to sufficient size in the course of next three weeks.

4.2.2 X-Ray crystal structure determinations. X-Ray intensities were measured on a Nonius KappaCCD diffractometer with a rotating anode and a graphite monochromator ($\lambda = 0.71073$ Å) at a temperature of 150(2) K. Intensity data were integrated with the Eval4⁷³ (assembly **9-L2**) or HKL2000⁷⁴ (assembly **9-L3**) software. Absorption correction and scaling was performed with SADABS.⁷⁵ The structures were solved with Direct Methods using the programs SHELXS-97⁷⁶ (assembly **9-L2**) or SIR-97⁷⁷ (assembly **9-L3**). Both structures were refined with SHELXL-97⁷⁶ against F² of all reflections. Hydrogen atoms were introduced in calculated positions and refined with a riding model. Geometry calculations and checking for higher symmetry was performed with the PLATON program.⁷⁸

4.2.2.1 Assembly 9-L2. C₃₁H₃₂N₇PS₂Zn, $M_w = 663.10$, yellow needle, $0.20 \times 0.08 \times 0.06$ mm³, triclinic, $P\bar{1}$, $a = 11.1142(8)$, $b = 11.1774(9)$, $c = 13.0986(8)$ Å, $\alpha = 81.434(3)^\circ$, $\beta = 94.669(4)^\circ$, $\gamma = 78.433(2)^\circ$, $V = 1573.1(2)$ Å³, $Z = 2$, $D_c = 1.400$ g cm⁻³, $\mu = 1.00$ mm⁻¹. 13454 reflections were measured up to a resolution of $(\sin\theta/\lambda)_{\max} = 0.50$ Å⁻¹. A large anisotropic mosaicity of 1.6° was used for the integration of this weakly diffracting crystal. 3373 Reflections were unique ($R_{\text{int}} = 0.056$), of which 2429 were observed ($I > 2\sigma(I)$). 383 parameters were refined with no restraints. $R1/wR2$ ($I > 2\sigma(I)$): 0.0867/0.1990. $R1/wR2$ (all refl.): 0.1219/0.2191. $S = 1.071$. Residual electron density between 0.56 and 2.23 e Å⁻³.

4.2.2.2 Assembly 9-L3. C₃₁H₃₂N₇PS₂Zn·C₇H₈, $M_w = 755.23$, orange triangular prism, $0.36 \times 0.27 \times 0.21$ mm³, triclinic, $P\bar{1}$, $a = 12.9582(3)$, $b = 13.0266(2)$, $c = 13.1409(3)$ Å, $\alpha = 115.9892(8)^\circ$, $\beta = 93.8687(10)^\circ$, $\gamma = 107.0963(9)^\circ$, $V = 1855.38(7)$ Å³, $Z = 2$, $D_x = 1.352$ g cm⁻³, $\mu = 0.85$ mm⁻¹. 21422 Reflections were measured up to a resolution of $(\sin\theta/\lambda)_{\max} = 0.57$ Å⁻¹. 5715 Reflections were unique ($R_{\text{int}} = 0.045$), of which 4719 were observed ($I > 2\sigma(I)$). 447 Parameters were refined with no restraints. $R1/wR2$ ($I > 2\sigma(I)$): 0.0616/0.1526. $R1/wR2$ (all refl.): 0.0758/0.1615. $S = 1.037$. Residual electron density between 0.56 and 1.18 e Å⁻³.

4.3 UV-Vis titration

To 2.500 ml 50.0 $\times 10^{-6}$ mol l⁻¹ solution of complex **11** in a quartz cuvette, aliquots (5 μ l for first 25 points, 10 μ l for all following points) of 2.50 $\times 10^{-3}$ mol l⁻¹ solution of pyridine were added. After each addition, the solution was shaken, left to equilibrate for 1 min and a UV-Vis spectrum was recorded. A blue-shift of the band at 487 nm and of the valley at 420 nm, as well as the appearance of the new absorption band at 343 nm were observed upon addition of pyridine. Absorbance values at

Table 2 Concentrations and amounts of compounds used in catalytic experiments

Compound	equiv.	$c/(10^{-3}\text{ mol l}^{-1})$	$m\text{ mg}^{-1}$ or V
Rh(acac)(CO) ₂	1.00	0.70	0.903
LI	5.00	3.50	4.59
L2 or L3	5.00	3.50	4.61
L4	5.00	3.50	4.64
1-Octene	1000	700	550/ μl
2- or 3-Octene	500	350	275 μl
Zn(btsc) 9	5(15)	3.50(10.5)	6.98 (20.9)
Zn(btsc) 10	5(15)	3.50(10.5)	5.91 (17.7)
Zn(btsc) 11	5(15)	3.50(10.5)	9.80 (29.4)

529 nm were taken to create plot ($A_0 - A$) vs. C_{pyridine} , shown in insert in Fig. 3. The binding constant was calculated using the curve fitting procedure for the 1:1 complexation case, developed in the Hunter Group⁵⁰ by having A_{end} and K as unknowns, what resulted with $A_0 - A_{\text{end}} = 0.0826771$ and $K = (1.4 \pm 0.2) 10^5 \text{ l mol}^{-1}$. The fitting using in-house developed curve-fitting scripts gave value of $(1.6 \pm 0.1) \times 10^5$, which was more accurate and therefore given in the text.

4.4 High-pressure infrared spectroscopy

The autoclave built for *in situ* infrared spectroscopy (described in detail by van Leeuwen *et al.*),⁵⁷ was cleaned, dried, tested for leaks (pressurised with 40 bar hydrogen for 16 h), and flushed (3×15 bar) with syngas prior to use. All handling and manipulations were performed under oxygen and water-free atmosphere (Ar of 1 bar 1:1 syngas). Only freshly dried and degassed liquids were used. 1-Octene was additionally purified by filtration over a short plug of alumina.

4.4.1 HP-IR experiment with the supramolecular ligand.

The Zn(btsc) complex **9** was weighed (93.85 mg, 235.2 μmol , 14.2 equiv.) in air, transferred into a Schlenk-tube, and repeatedly evacuated and flushed with Ar. 10.0 ml dichloromethane (DCM) and a solution of **L4** (20.8 mg, 78.4 μmol , 4.7 equiv.) in 1.0 ml DCM were added to it. The mixture was stirred at room temperature for 30 min, and then transferred into the IR-autoclave. The Schlenk-tube was washed with 3.0 ml DCM, which was added to the mixture in the autoclave, which was then again flushed (3×15 bar) with syngas and pressurised to 19 bar. The injection chamber of the autoclave was charged with solution of Rh(acac)(CO)₂ (4.283 mg, 16.6 μmol , 1 equiv.) in 1 ml DCM and pressurised to 30 bar. The autoclave was heated to 40 °C (the pressure increased to about 20.5 bar). Background spectrum was taken *ca.* 1 h after the temperature reached 40 °C, and then the solution of rhodium precursor was injected. The injection chamber was cleaned, dried, charged with 1.0 ml 1-octene solution (521 μl , 3.32 mmol, 200 equiv.) and pressurised again with *ca.* 30 bar syngas. The incubation was followed all the while. The frequencies around 2000 cm^{-1} stopped changing *ca.* 45 min after rhodium precursor injection. Four bands (2071, 2056, 2005 and 1970 cm^{-1}) were observed, indicating mixture of two (eq-eq and eq-ap, see main text) rhodium hydride species. In the region of the CO-bridged Rh-dimers no signal appears initially, however, small signals start appearing about two hours after the

completed incubation, indicating slow transformation of the hydride species into the inactive rhodium dimeric species. Therefore, in separate experiment the substrate was injected 60 min after Rh(acac)(CO)₂ was added, and the reaction monitored. The band of the aldehyde-CO at 1722 cm^{-1} started growing immediately, and the band of the C=C bond (1639 cm^{-1}) diminished. During the catalysis (18 h) a weak shoulder at 1986 cm^{-1} could be observed, possibly the vibration of the the CO-bridged dirhodium species, whose corresponding signal at *ca.* 1790 cm^{-1} was observed before the aldehyde band covered it. The signal of the dinuclear rhodium species stayed constant at low intensity all the time during catalysis, suggesting that it was in the equilibrium with the catalytically active rhodium species.

4.4.2 HP-IR using triphenylphosphine as ligand. This experiment was performed analogously to the previously described one. No Zn complex was added. The amounts of ligand and rhodium precursor used: triphenylphosphine 25 mg (95.3 μmol , 5 equiv.), Rh(acac)(CO)₂ 4.920 mg (19.10 μmol , 1 equiv.). The substrate was, however, not added, only the formation of the hydride species was monitored. Like in the above case, four main bands were observed, however, at lower frequencies (2056, 2030, 1989 and 1941 cm^{-1}). In addition to them, the signals of the dinuclear rhodium species start appearing soon after rhodium injection and are present in significant amount (we estimate up to 30% of all rhodium is in form of dimers, based on the relative intensities of the bands in IR).

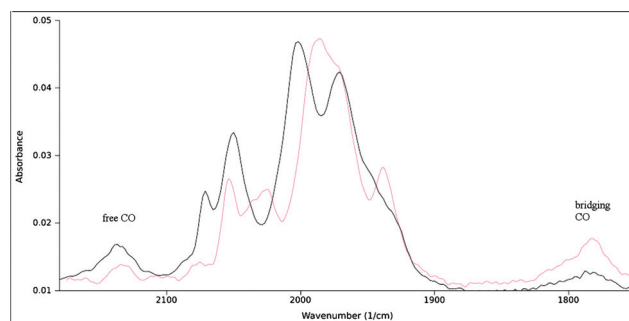


Fig. 12 Comparison of the HP-FTIR spectra of the rhodium species formed with the supramolecular ligand **L4-93** (black line) and triphenylphosphine (**LI**, magenta line). Use of only **L4** or **LI** with 3 equivalents of complex **9** leads to spectra (not shown here) identical to the one obtained with **LI**.

4.5 Catalysis

The Zn(btsc) complexes were weighed directly into the glass inlays before the autoclaves were assembled. After closing, the autoclaves were charged respectively with solutions of the ligand (s), Rh(acac)(CO)₂, and the substrate (for the exact amounts see Table 2). Toluene was added at the end to fill the total reaction volume to 5 ml. The charged autoclave was flushed three times with 30–35 bar syngas (CO/H₂ = 1:1), pressurized to 20 bar and lowered into the previously warmed (40 °C) oil bath. After 16 or 24 h, the pressure was released, autoclave cooled, rinsed with nitrogen and the reaction quenched with tributylphosphite (0.5 ml in each reactor). The raw reaction mixture was diluted

with DCM (2–3 drops of reaction mixture per GC vial) and injected into the GC.

Acknowledgements

This research was financially supported by the EU - Marie Curie Research and Training Network RevCat, and Dutch National School Combination Catalysis Controlled by Chemical Design (NRSC-Catalysis).

References

‡ In order to prevent demetallation of the Zn(II)(salphens) and Zn(II)porphyrins during hydroformylation, an excess of a non-coordinating nitrogen base, diisopropyl-ethylamin (DIPEA), is routinely added to the reaction mixture.

§ The ligands **L2**–**L4** (Fig. 3a) are routinely used as templates for construction of supramolecular transition metal catalysts. The position of nitrogen donor in **L2** and **L3** allows creation of qualitatively different steric bulk upon coordination of a Zn(II) complex to N. Further, the electronic effects of N in these positions influence the electronic properties of the phosphorous atom, creating slight differences in electron density on the transition metal during catalysis, which in turn, may be manifested as slight differences in activity. The *ortho* analogue of these complexes is not used, due to its low association constant, caused by steric bulk (the diphenylphosphino-moiety close to N).

¶ Catalyst activation, Fig. 5, under typically 20 bar syngas, CO/H₂ = 1 : 1, usually leads to formation of mixture of bis-phosphine rhodiumhydride species, eq–eq or *ee*, and eq–ap or *ea*.⁵⁶ Each of these isomers produces two characteristic CO-bands in the infrared spectrum, leading to total of four bands when both isomers are present in solution.

|| No nitrogen base was added, what is typical when Zn(salphens) and Zn(porphyrins) are used as building blocks.

** In type I kinetics, the reaction rate order in respect to the substrate is 1, and the rate-limiting, as well as the rate-determining step are early in the catalytic cycle, while in the type II kinetics the rate order with respect to the substrate is zero and hydrogenolysis is the rate-limiting step.^{62,63}

†† CO coordinated to Rh or, less probable, to the CO of the Rh–acyl moiety.

‡‡ The pipette was previously sealed at the thin end and set within a Schlenk-tube under an inert atmosphere.

- 1 J.-M. Lehn, *Science*, 2002, **295**, 2400–3.
- 2 J.-M. Lehn, *Chem. Soc. Rev.*, 2007, **36**, 151–60.
- 3 E. C. Constable, *Chem. Soc. Rev.*, 2007, **36**, 246–53.
- 4 D. Fiedler, D. H. Leung, R. G. Bergman and K. N. Raymond, *Acc. Chem. Res.*, 2005, **38**, 349–58.
- 5 M. Fujita, M. Tominaga, A. Hori and B. Therrien, *Acc. Chem. Res.*, 2005, **38**, 369–78.
- 6 B. Champin, P. Mobian and J.-P. Sauvage, *Chem. Soc. Rev.*, 2007, **36**, 358–66.
- 7 S. J. Loeb, *Chem. Soc. Rev.*, 2007, **36**, 226–35.
- 8 S. Saha and J. F. Stoddart, *Chem. Soc. Rev.*, 2007, **36**, 77–92.
- 9 M. Eddaoudi, D. B. Moler, H. Li, B. Chen, T. M. Reineke, M. O’Keeffe and O. M. Yaghi, *Acc. Chem. Res.*, 2001, **34**, 319–330.
- 10 L. Brammer, *Chem. Soc. Rev.*, 2004, **33**, 476–89.
- 11 A. K. Cheetham, C. N. R. Rao and R. K. Feller, *Chem. Commun.*, 2006, 4780.
- 12 H. Furukawa, J. Kim, N. W. Ockwig, M. O’Keeffe and O. M. Yaghi, *J. Am. Chem. Soc.*, 2008, **130**, 11650–61.
- 13 C. Valente, E. Choi, M. E. Belowich, C. J. Doonan, Q. Li, T. B. Gasa, Y. Y. Botros, O. M. Yaghi and J. F. Stoddart, *Chem. Commun.*, 2010, **46**, 4911–4913.
- 14 N. L. Rosi, J. Eckert, M. Eddaoudi, D. T. Vodak, J. Kim, M. O’Keeffe and O. M. Yaghi, *Science*, 2003, **300**, 1127–9.
- 15 Y.-F. Song and L. Cronin, *Angew. Chem., Int. Ed.*, 2008, **47**, 4635–7.
- 16 M. Latroché, S. Surble, C. Serre, C. Mellot-Draznieks, P. L. Llewellyn, J.-H. Lee, J.-S. Chang, S. H. Jung and G. Férey, *Angew. Chem., Int. Ed.*, 2006, **45**, 8227–31.
- 17 Y. Li and R. T. Yang, *J. Am. Chem. Soc.*, 2006, **128**, 726–7.
- 18 F. Nouar, J. F. Eubank, T. Bousquet, L. Wojtas, M. J. Zaworotko and M. Eddaoudi, *J. Am. Chem. Soc.*, 2008, **130**, 1833–5.
- 19 Q. Li, W. Zhang, O. S. Miljanić, C.-H. Sue, Y.-L. Zhao, L. Liu, C. B. Knobler, J. F. Stoddart and O. M. Yaghi, *Science*, 2009, **325**, 855–9.
- 20 H.-L. Jiang, Y. Tatsu, Z.-H. Lu and Q. Xu, *J. Am. Chem. Soc.*, 2010, **132**, 5586–7.
- 21 C.-D. Wu and W. Lin, *Angew. Chem., Int. Ed.*, 2007, **46**, 1075–8.
- 22 A. M. Shultz, O. K. Farha, J. T. Hupp and S. T. Nguyen, *J. Am. Chem. Soc.*, 2009, **131**, 4204–5.
- 23 *Supramolecular Catalysis*, ed. P. W. N. M. van Leeuwen, Wiley VCH Verlag GmbH & Co, Weinheim, 2008.
- 24 J. E. Falk, *Porphyrins and Metalloporphyrins*, Elsevier Publishing Co., Amsterdam, 1964.
- 25 V. F. Slagt, J. N. H. Reek, P. C. J. Kamer and P. W. N. M. van Leeuwen, *Angew. Chem., Int. Ed.*, 2001, **40**, 4271–274.
- 26 V. F. Slagt, P. C. J. Kamer, P. W. N. M. van Leeuwen and J. N. H. Reek, *J. Am. Chem. Soc.*, 2004, **126**, 1526–36.
- 27 M. Kuil, T. Soltner, P. W. N. M. van Leeuwen and J. N. H. Reek, *J. Am. Chem. Soc.*, 2006, **128**, 11344–5.
- 28 A. M. Kluwer, R. Kapre, F. Hartl, M. Lutz, A. L. Spek, A. M. Brouwer, P. W. N. M. van Leeuwen and J. N. H. Reek, *Proc. Natl. Acad. Sci. USA*, 2009, **106**, 10460–10465.
- 29 J. Flapper and J. N. H. Reek, *Angew. Chem., Int. Ed.*, 2007, **46**, 8590–2.
- 30 A. W. Kleij, M. Kuil, D. M. Tooke, M. Lutz, A. L. Spek and J. N. Reek, *Chem.–Eur. J.*, 2005, **11**, 4743–50.
- 31 E. C. Escudero-Adán, J. Benet-Buchholz and A. W. Kleij, *Inorg. Chem.*, 2007, **46**, 7265–7.
- 32 E. C. Escudero-Adán, J. Benet-Buchholz and A. W. Kleij, *Inorg. Chem.*, 2008, **47**, 410–2.
- 33 K. Jensen and E. Rancke-Madsen, *Z. Anorg. Allg. Chem.*, 1934, **219**, 243–255.
- 34 G. Bähr, *Z. Anorg. Allg. Chem.*, 1952, **268**, 351–363.
- 35 G. Bähr, *Z. Anorg. Allg. Chem.*, 1953, **273**, 325–332.
- 36 H. G. Petering, H. H. Buskirk and G. E. Underwood, *Cancer Res.*, 1964, **24**, 367–72.
- 37 D. H. Petering, *Bioinorg. Chem.*, 1972, **1**, 255–271.
- 38 M. Campbell, *Coord. Chem. Rev.*, 1975, **15**, 279–319.
- 39 A. R. Cowley, J. R. Dilworth, P. S. Donnelly, E. Labisbal and A. Sousa, *J. Am. Chem. Soc.*, 2002, **124**, 5270–5271.
- 40 J. L. J. Dearling and P. J. Blower, *Chem. Commun.*, 1998, 2531–2532.
- 41 R. L. Aft, J. S. Lewis, F. Zhang, J. Kim and M. J. Welch, *Cancer Res.*, 2003, **63**, 5496–504.
- 42 S. I. Pascu, P. A. Waghorn, T. D. Conry, B. Lin, H. M. Betts, J. R. Dilworth, R. B. Sim, G. C. Churchill, F. I. Aigbirhio and J. E. Warren, *Dalton Trans.*, 2008, 2107–10.
- 43 A. R. Cowley, J. R. Dilworth, P. S. Donnelly, J. M. Heslop and S. J. Ratcliffe, *Dalton Trans.*, 2007, 209–17.
- 44 M. Christlieb, A. R. Cowley, J. R. Dilworth, P. S. Donnelly, B. M. Paterson, H. S. R. Struthers and J. M. White, *Dalton Trans.*, 2007, 327–31.
- 45 M. Christlieb, H. S. R. Struthers, P. D. Bonnitcha, A. R. Cowley and J. R. Dilworth, *Dalton Trans.*, 2007, 5043–54.
- 46 A. W. Kleij and J. N. H. Reek, *Chem.–Eur. J.*, 2006, **12**, 4218–27.
- 47 A. W. Kleij, M. Kuil, D. M. Tooke, M. Lutz, A. L. Spek and J. N. H. Reek, *Chem.–Eur. J.*, 2005, **11**, 4743–50.
- 48 A. W. Kleij, M. Kuil, D. M. Tooke, A. L. Spek and J. N. H. Reek, *Inorg. Chem.*, 2005, **44**, 7696–8.
- 49 M. Kuil, E. P. Goudriaan, A. W. Kleij, D. M. Tooke, A. L. Spek, P. W. N. M. van Leeuwen and J. N. H. Reek, *Dalton Trans.*, 2007, 2311–20.
- 50 P. A. Bisson, C. A. Hunter, C. J. Morales and K. Young, *Chem.–Eur. J.*, 1998, **4**, 845–851.
- 51 *Analytical Methods in Supramolecular Chemistry*, ed. C. A. Shalley, Wiley VCH Verlag GmbH & Co, Weinheim, 2007.
- 52 L. Alsop, A. Cowley, J. Dilworth, P. Donnelly, J. Peach and J. Rider, *Inorg. Chim. Acta*, 2005, **358**, 2770–2780.
- 53 C. A. Hunter and J. K. M. Sanders, *J. Am. Chem. Soc.*, 1990, **112**, 5525–5534.
- 54 S. Grimme, *Angew. Chem., Int. Ed.*, 2008, **47**, 3430–4.
- 55 P. W. N. M. van Leeuwen, in *Introduction to hydroformylation*, ed. P. W. N. M. van Leeuwen and C. Claver, Kluwer Academic Publishers, Amsterdam, 2000, ch. 1, pp. 1–13.
- 56 P. C. J. Kamer, P. W. N. M. van Leeuwen and J. N. H. Reek, *Acc. Chem. Res.*, 2001, **34**, 895–904.
- 57 P. C. J. Kamer, A. V. Rooy, G. C. Schoemaker and P. W. N. M. van Leeuwen, *Coord. Chem. Rev.*, 2004, **248**, 2409–2424.

- 58 L. Damoense, M. Datt, M. Green and C. Steenkamp, *Coord. Chem. Rev.*, 2004, **248**, 2393–2407.
- 59 L. a. van der Veen, P. H. Keeven, G. C. Schoemaker, J. N. H. Reek, P. C. J. Kamer, P. W. N. M. van Leeuwen, M. Lutz and A. L. Spek, *Organometallics*, 2000, **19**, 872–883.
- 60 K. Nozaki, T. Matsuo and F. Shibahara, *Organometallics*, 2003, **22**, 594–600.
- 61 A. W. Kleij, M. Lutz, A. L. Spek, P. W. N. M. van Leeuwen and J. N. H. Reek, *Chem. Commun.*, 2005, 3661–3.
- 62 P. C. J. Kamer, J. N. H. Reek and P. W. N. M. van Leeuwen, in *Rhodium Phosphite Catalysts*, ed. P. W. N. M. van Leeuwen, Kluwer Academic Publishers, Amsterdam, 2000, ch. 3, pp. 35–62.
- 63 P. W. N. M. van Leeuwen, C. P. Casey and G. T. Whiteker, in *Phosphines as ligands*, ed. P. W. N. M. van Leeuwen and C. Claver, Kluwer Academic Publishers, Amsterdam, 2000, ch. 4, pp. 63–105.
- 64 P. W. N. M. van Leeuwen and C. F. Roobeek, *J. Organomet. Chem.*, 1983, **258**, 343–350.
- 65 A. van Rooy, E. N. Orij, P. C. J. Kamer and P. W. N. M. van Leeuwen, *Organometallics*, 1995, **14**, 34–43.
- 66 B. G. Van den Hoven and H. Alper, *J. Org. Chem.*, 1999, **64**, 3964–3968.
- 67 S. Deerenberg, P. C. J. Kamer and P. W. N. M. van Leeuwen, *Organometallics*, 2000, **19**, 2065–2072.
- 68 S. a. Moteki, D. Wu, K. L. Chandra, D. S. Reddy and J. M. Takacs, *Org. Lett.*, 2006, **8**, 3097–100.
- 69 E. Zuidema, L. Escorihuela, T. Eichelsheim, J. J. Carbó, C. Bo, P. C. J. Kamer and P. W. N. M. van Leeuwen, *Chem.–Eur. J.*, 2008, **14**, 1843–53.
- 70 A. M. Kluwer, I. Ahmad and J. N. H. Reek, *Tetrahedron Lett.*, 2007, **48**, 2999–3001.
- 71 E. F. Pettersen, T. D. Goddard, C. C. Huang, G. S. Couch, D. M. Greenblatt, E. C. Meng and T. E. Ferrin, *J. Comput. Chem.*, 2004, **25**, 1605–12.
- 72 R. W. Bost and W. F. Smith, *J. Am. Chem. Soc.*, 1931, **53**, 652–654.
- 73 A. J. M. Duisenberg, L. M. J. Kroon-Batenburg and A. M. M. Schreurs, *J. Appl. Crystallogr.*, 2003, **36**, 220–229.
- 74 Z. Otwinowski and W. Minor, in *Methods in Enzymology, Volume 276*, ed. J. C. W. Carter and R. M. Sweets, Academic Press, 1997, pp. 307–326.
- 75 G. M. Sheldrick, *SADABS*, Universität Gottingen, Germany.
- 76 G. M. Sheldrick, *Acta Cryst.*, 2008, **A64**, 112–22.
- 77 A. Altomare, M. C. Burla, M. Camalli, G. L. Cascarano, C. Giacovazzo, A. Guagliardi, A. G. Moliterni, G. Polidori and R. Spagna, *J. Appl. Crystallogr.*, 1999, **32**, 115–119.
- 78 A. L. Spek, *Acta Cryst.*, 2009, **D65**, 148–55.